

# Extreme diversity in noncalcifying haptophytes explains a major pigment paradox in open oceans

Hui Liu<sup>a,b</sup>, Ian Probert<sup>a</sup>, Julia Uitz<sup>c</sup>, Hervé Claustre<sup>d</sup>, Stéphane Aris-Brosou<sup>e</sup>, Miguel Frada<sup>b</sup>, Fabrice Not<sup>a</sup>, and Colomán de Vargas<sup>a,b,1</sup>

<sup>a</sup>Centre National de la Recherche Scientifique, Unité Mixte de Recherche 7144 and Université Pierre et Marie Curie Paris 06, Equipe Evolution du Plancton et Paléo-Océans, Station Biologique de Roscoff, 29682, France; <sup>b</sup>Institute of Marine and Coastal Sciences, Rutgers University, New Brunswick, NJ 08901; <sup>c</sup>Marine Physical Laboratory, Scripps Institution of Oceanography, University of California at San Diego, La Jolla, CA 92093-0238; <sup>d</sup>Centre National de la Recherche Scientifique, Unité Mixte de Recherche 7093 and Université Pierre et Marie Curie Paris 06, Laboratoire d'Océanographie de Villefranche/Mer, 06234, France; and <sup>e</sup>Department of Biology and Department of Mathematics and Statistics, University of Ottawa, Ottawa, ON, Canada K1N 6N5

Communicated by W. A. Berggren, Woods Hole Oceanographic Institution, Woods Hole, MA, June 2, 2009 (received for review December 18, 2008)

The current paradigm holds that cyanobacteria, which evolved oxygenic photosynthesis more than 2 billion years ago, are still the major light harvesters driving primary productivity in open oceans. Here we show that tiny unicellular eukaryotes belonging to the photosynthetic lineage of the Haptophyta are dramatically diverse and ecologically dominant in the planktonic photic realm. The use of Haptophyta-specific primers and PCR conditions adapted for GC-rich genomes circumvented biases inherent in classical genetic approaches to exploring environmental eukaryotic biodiversity and led to the discovery of hundreds of unique haptophyte taxa in 5 clone libraries from subpolar and subtropical oceanic waters. Phylogenetic analyses suggest that this diversity emerged in Paleozoic oceans, thrived and diversified in the permanently oxygenated Mesozoic Panthalassa, and currently comprises thousands of ribotypic species, belonging primarily to low-abundance and ancient lineages of the "rare biosphere." This extreme biodiversity coincides with the pervasive presence in the photic zone of the world ocean of 19'-hexanoyloxyfucoxanthin (19-Hex), an accessory photosynthetic pigment found exclusively in chloroplasts of haptophyte origin. Our new estimates of depth-integrated relative abundance of 19-Hex indicate that haptophytes dominate the chlorophyll *a*-normalized phytoplankton standing stock in modern oceans. Their ecologic and evolutionary success, arguably based on mixotrophy, may have significantly impacted the oceanic carbon pump. These results add to the growing evidence that the evolution of complex microbial eukaryotic cells is a critical force in the functioning of the biosphere.

Haptophyta | photosynthesis | protistan biodiversity | eukaryotic biodiversity

Oxygenic photosynthesis, the most complex and energetically powerful molecular process in biology, originated in cyanobacteria more than 2 billion years ago in Archean oceans (1). Marine photosynthesis still contributes  $\approx 50\%$  of total primary production on Earth (2). This revolutionary process was integrated, at least once, into an ancestral phagotrophic eukaryotic lineage through the evolution of chloroplasts, which themselves were redistributed to a large variety of aquatic eukaryote lineages via permanent secondary and tertiary endosymbioses (3). Despite this evolutionary trend from photosynthetic prokaryotes to eukaryotes, particularly visible in today's coastal oceans where microalgae such as diatoms and dinoflagellates are omnipresent, cyanobacteria have been repeatedly claimed as the champions of photosynthesis in open ocean waters (4). This hypothesis followed the introduction of flow cytometry and molecular genetic approaches to biological oceanography in the 1980s, which revealed astonishing concentrations of minute cyanobacterial cells of the genera *Prochlorococcus* and *Synechococcus* in marine waters (5). The physiology, ecology, and functional and environmental genomics of these prokaryotes are subjects of ongoing intensive study (6).

Several lines of evidence in fact argue for eukaryotic supremacy over marine oxygenic photosynthesis. Flow cytometric cell counts (7) show that picophototrophic protists ( $0.2\text{--}3\ \mu\text{m}$  cell size) are indeed 1–2 orders of magnitude less abundant than cyanobacteria. However, biophysical and group-specific <sup>14</sup>C-uptake measurements suggest that tiny eukaryotes can, through equivalent or higher growth rates of relatively larger cells, dominate carbon biomass and net production in both coastal (8) and oceanic (7) settings. High performance liquid chromatography (HPLC) analyses of group-specific accessory pigments have further stressed the ecologic prevalence of phototrophic protist taxa. In particular, 19'-hexanoyloxyfucoxanthin (19-Hex) was originally estimated to account for 20–50% of total chlorophyll *a* (Chl*a*) biomass in tropical Atlantic and Pacific sites (9) and has since been consistently reported in open ocean photic-zone waters, e.g., (10, 11), suggesting a ubiquitous occurrence of haptophytes in upper layers of the water column. Surveys of genetic diversity based on environmental ribosomal DNA libraries over the last decade have unveiled an unexpected diversity of tiny eukaryotes in all oceans (12). Paradoxically, most picoeukaryotic sequence diversity from photic layers represented novel *heterotrophic* (13) and *parasitic* (14) protists within phyla traditionally thought to be dominated by photoautotrophs. This bias indicated that marine protist diversity might be significantly skewed toward heterotrophic taxa (15), as appears to be the case for prokaryotes. However, the paucity of haptophyte nuclear rDNA sequences in these surveys contrasts strikingly with the abundance of 19-Hex in marine waters.

Here we use a combination of previously undescribed genetic, pigment, and microscopy data to unveil a dramatic and ancient diversity of unique photosynthetic picoplanktonic protists within the Haptophyta. This diversity could account for the mysteriously high concentration of 19-Hex in the photic layer of the world oceans, our calculations indicating that haptophytes contribute  $\approx 2$ -fold more than either cyanobacteria or diatoms to global oceanic Chl*a* standing stock. The phylogenetic position of these tiny haptophytes implies that they are photophagotrophic, coinciding with the recent discovery of dominant bacterivory by small eukaryotic phytoplankton in the oceans (16). Mixotrophy may provide a competitive advantage over both purely phototrophic microalgae (including cyanobacteria) and aplastidial protists, and the extreme genetic diversity of tiny haptophytes matches the cellular and behavioral complexity inherent in this mixed mode of nutrition.

Author contributions: C.d.V. designed research; H.L., I.P., J.U., H.C., M.F., and F.N. performed research; H.L., J.U., H.C., S.A.-B., F.N., and C.d.V. analyzed data; and I.P. and C.d.V. wrote the paper.

The authors declare no conflict of interest.

<sup>1</sup>To whom correspondence should be addressed. E-mail: vargas@sb-roscoff.fr.

This article contains supporting information online at [www.pnas.org/cgi/content/full/0905841106/DCSupplemental](http://www.pnas.org/cgi/content/full/0905841106/DCSupplemental).

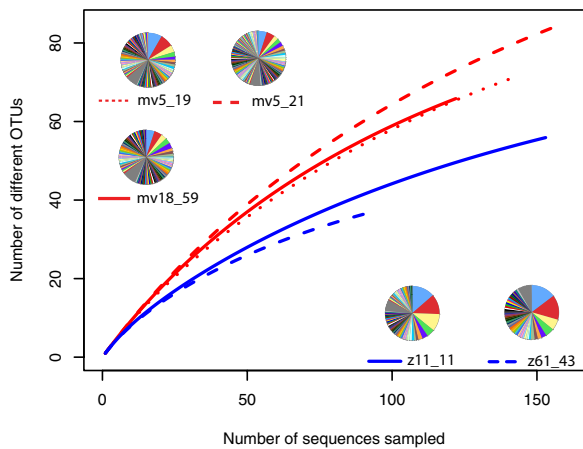


**Fig. 1.** Rarefaction analysis for each environmental clone library based on unique LSU rDNAs sequences (OTUs); 72, 85, 65, 56, and 37 OTUs, respectively, were obtained from the Indian ocean (Mv 19, 21, 18) and subarctic (z 11, 43) clone libraries (Fig. S1). The pie charts show, for each library, the amount of identical sequences in each retrieved OTU.

**Results and Discussion**

**A Massive Unique Diversity of Oceanic Picohaptophytes.** We first show that previous nuclear rDNA PCR-based studies of eukaryotic communities were subject to severe selective amplification biases. Several groups of protists known to have long and/or GC-rich rDNA are virtually missing from environmental clone libraries produced by classical PCR amplification protocols using “general eukaryote” SSU rDNA primers (12, 13). This is the case for the haptophytes, the rDNA of which has a mean GC content of  $\approx 57\%$ . We therefore used haptophyte-specific primers and a PCR protocol designed for GC-rich genomes to amplify LSU rDNA D1–D2

fragments from bulk DNA extracted from the 0.2- to 3- $\mu\text{m}$  fraction of seawater collected at 4 offshore stations in the Arctic and Indian oceans (Fig. S1, Table S1). Standard eukaryotic rDNA analyses of these samples yielded  $\approx 0.4\text{--}0.7\%$  haptophyte sequences (10, 11). In contrast, our data reveal hundreds of previously undescribed rDNA sequences from tiny haptophytes. Rarefaction curves for individual clone libraries (Fig. 1) indicate that current sequencing effort is far from exhaustive, notably in subtropical waters where genetic diversity is particularly dramatic. Estimates of the number of unique ribotypes using the Chao1 estimator were 1098–1147 and 325–509, respectively, for the Indian and Arctic ocean samples (with rather large confidence intervals, see Table S2). The frequency distribution of unique ribotypes (Fig. 1) indicates higher species richness in subtropical waters, with a substantial number of orphan and deep-branching genotypes (see below) in both warm and cold waters. This parallels recent observations for marine prokaryotes of a “seed bank” of ancient and rare taxa, termed the “rare biosphere” (17).

**Taxonomy and Evolutionary History of the Previously Undescribed Diversity.** The 674 novel environmental LSU rDNA sequences were aligned with 64 orthologous gene sequences from clonal culture strains representing a cross-section of known haptophyte biodiversity. Phylogenetic analyses indicate that all environmental sequences belong to the Haptophyta (Fig. 2), a eukaryotic phytoplankton division classically considered as nanoplankton (3–20  $\mu\text{m}$ ) and including the calcifying coccolithophores (18). However, not a single environmental sequence was strictly identical to any of the taxonomically defined sequences. The vast majority of environmental sequences form new clusters branching deep in the haptophyte phylogeny, most being related to *Chrysochromulina* species from clade B2 within the order Prymniales (19). The described representatives of this clade are nanoplanktonic and known almost exclusively from coastal and shelf environments (20); our data show they are in fact derived

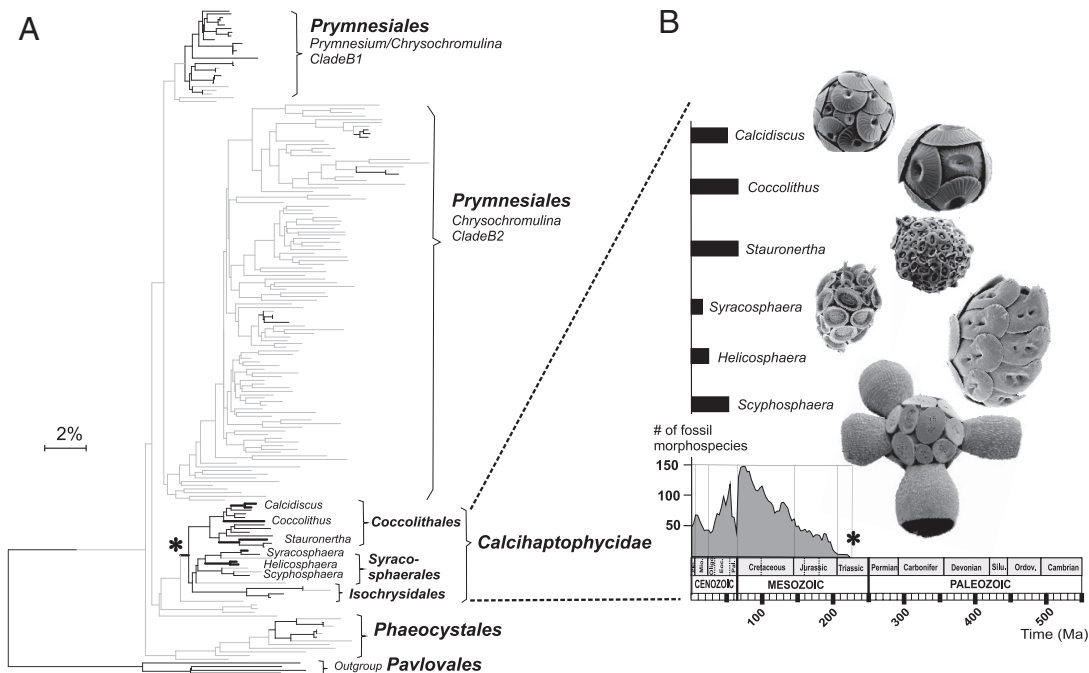


**Fig. 2.** Phylogenetic assessment of the previously undescribed haptophyte environmental diversity. (A) LSU rDNA tree (5% divergence cutoff) including environmental sequences (gray branches) and a taxonomic cross-section of cultured haptophyte taxa (black branches, see Table S3 for species identification). (B) Focus on the stratigraphic ranges (black rectangles) of key genera within the calcifying haptophytes (18) (thick black branches in the tree in A, and SEM images in B). The coccolithophore fossil record (50) (Lower Right) represents number of fossil morphospecies along time in millions of years. Black clover symbols indicate the origin of haptophyte calcification  $\approx 220$  Ma. Note that *Stauronertha* is the new genus name for *Cruciplacolithus* (51).

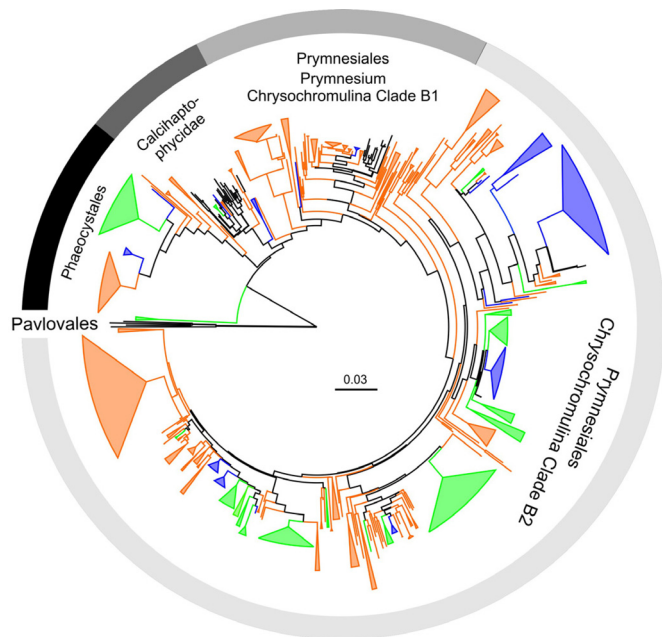


**Fig. 3.** Biogeographic partitioning of environmental tiny haptophyte diversity. This maximum likelihood tree contains all 674 environmental LSU rDNA sequences, with clustering above 97% similarity. Color code: orange, subtropical; blue, subpolar; green, both subpolar and subtropical; black external branches, taxonomically defined sequences from cultured haptophyte strains. Color code applies to internal branches when they are part of strictly subtropical or subpolar monophyletic groups.

from open ocean picoplanktonic taxa (Fig. 2). Note that the 2 other major prymnesiophyte lineages, the Phaeocystales and the Calcihaptophyceae (18), also appear to emerge from clusters of picohaptophyte sequences.

Calibration of our tree with the stratigraphic record of coccolithophore taxa (Fig. 2B) suggests that tiny haptophyte biodiversity emerged more than 250 Ma, in Paleozoic oceans (Fig. S2), before the evolution of intracellular biomineralization in the Calcihaptophyceae, which according to both fossil and molecular clock data occurred  $\approx 220$  Ma (18). The phylogenetic depth of most picohaptophyte clades argues for a Mesozoic diversification of the group, which may have thrived in the newly permanently oxygenated and largely oligotrophic Panthalassic Ocean, conditions which served as a selection matrix for a wide range of chlorophyll *a* + *c* containing protists (21). Many genotypes or genotype clusters were found exclusively in either subarctic or subtropical oceans, supporting significant lineage partitioning between cold mixed and warmer stratified waters (Fig. 3). This phylogeographic distribution of ribotypes suggests that tropical waters were the original center of diversification, with biodiversity spreading secondarily into higher latitudes, a scenario that fits the putative early radiation of the group in the warm Panthalassa.

**Ecologic Relevance of the Picohaptophytes.** Our genetic survey positions the haptophytes as the most diverse group of picophototrophs in modern open oceans. Recent exploration of chloroplast SSU rDNA in pelagic (22) and coastal (23) environments supports this conclusion. Haptophytes dominate the emerging chloroplast view\* of marine tiny eukaryotic phytoplankton in terms of both diversity and abundance. In a year-round data set

\*Note that chloroplast genomes are typically not GC biased, meaning they are amenable to standard PCR protocols and may provide a more accurate view of the real phytoplanktonic diversity.

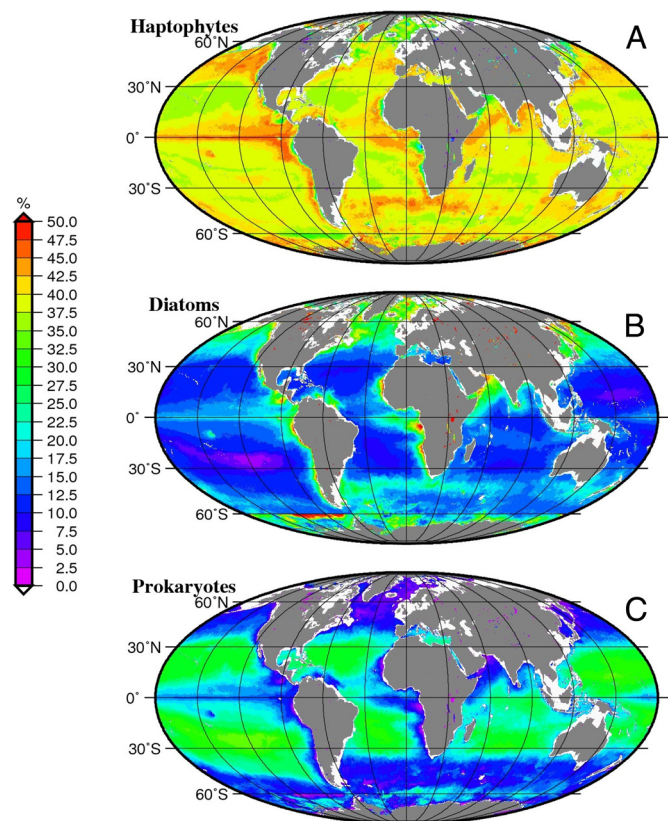


**Fig. 4.** Accessory pigments based on relative contribution of (A) haptophytes, (B) diatoms, and (C) photosynthetic prokaryotes to total chlorophyll-*a* biomass in the photic layer of the world ocean over the year 2000. The average yearly standing stocks associated with these 3 groups are respectively  $2.5 \times 10^9$ ,  $1.3 \times 10^9$ , and  $1.1 \times 10^9$  kg Chl*a*. See *Methods* for details of the calculation.

from the Gulf of Naples (23), >45% total and >70% unique eukaryote chloroplast rDNA sequences were of haptophyte origin, 55% of them belonging to the Prymnesiales clade-B2 (Fig. S3). This extreme diversity coincides with a numerical significance. Group-specific fluorescent *in situ* hybridization data from various oceanic settings indicate that haptophytes represent up to 35% of total picoeukaryotic cell numbers (24). Dot blot hybridizations using group-specific chloroplast rDNA probes indicated a mean dominance of  $\approx 45\%$  of haptophytes among other eukaryotic divisions during a 2-year survey of ultraphytoplankton ( $< 5 \mu\text{m}$  cell size) in Mediterranean waters (23). To assess whether these localized observations are representative of a global trend, we evaluated the contribution of haptophytes to oceanic phototrophic biomass using an empirical model based on >2,400 worldwide vertical profiles of HPLC pigment data integrated through monthly ocean-color composites of surface Chl*a* concentrations measured by the *SeaWiFS* satellite sensor in the year 2000 (Fig. 4). This analysis revealed that 19-Hex was the dominant accessory pigment in the oceans over this period, representing about twice the standing stocks of either fucoxanthin (diatoms) or zeaxanthin (prokaryotes) when normalized to Chl*a*. Haptophytes appear thus to represent the background oceanic light harvesters, contributing from 30 to 50% of total photosynthetic standing stock across the world ocean.

**Mixotrophy, the Key to the Success of Tiny Haptophytes in Open Oceans?** The phylogenetic position of the majority of the picohaptophytes in the Prymnesiales strongly suggests that they are mixotrophic, i.e., able to supplement their phototrophic regime with uptake and assimilation of organic nutrients. Laboratory experiments have shown that members of the Prymnesiales are

typically capable of ingesting organic particles and prey (e.g., refs. 25–27). Their third flagellum-like appendix, the haptonema, which is particularly long relative to cell size in all described members of Prymnesiales clade B2, can be used to catch preys and transfer them to the cell membrane for active phagocytosis (28). Even in calcihaptophytes, highly modified coccoliths may be involved in harvesting preys (29). Field studies on bacterivory by plastid-containing protists have demonstrated the dominance of tiny haptophyte-like cells in oceanic mixotrophy, e.g., see refs. 16 and 30. Recent quantitative evidence (16) revealed that eukaryotic algae with cell size  $\leq 5 \mu\text{m}$ , expected to be mostly haptophytes, carry out most of the bacterivory in the euphotic layer of both the temperate and tropical Atlantic Ocean. Furthermore, significant 19-Hex concentrations were recorded in 200- to 300-m-deep layers of the clearest waters on Earth in the South Pacific gyre (31), depths where irradiance at noon is not even sufficient for photosynthesis to cover basic cellular metabolic requirements. The complex combination of phagocytotic and photosynthetic modes of nutrition can be postulated to have allowed haptophytes to attain relatively large size and morphological complexity while maintaining prokaryote-like growth rates, and thus to have radiated into a wide diversity of ecogenotypes. The nutritional flexibility offered by mixotrophy is likely to have equipped the tiny haptophytes with a significant competitive advantage over both purely phototrophic and aplastidial cells under different light (depth) and nutrient regimes<sup>†</sup>.

**Concluding Remarks.** Besides their unanticipated diversity and abundance, the unveiled haptophytes display morphological features that suggest they play critical roles in organic carbon fluxes on a global scale. Size analyses of cells identified by haptophyte-specific fluorescent probes revealed a mode of  $\approx 4 \mu\text{m}$ , with largest sizes of 8–9  $\mu\text{m}$  (Fig. S4 and Table S4). In terms of volume, haptophytes are thus typically 300–3,000 times larger than *Prochlorococcus*, the most abundant marine cyanobacteria. The few available electron microscopy images of these open ocean tiny haptophytes indicate that they do produce organic plate scales (Fig. S5), a plesiomorphic character common to the overwhelming majority of prymnesiophytes. Interestingly, abundant and diverse *Chrysochromulina* spp. scales were recently observed in Atlantic surface sediments collected at 4,850 m (32). The taxonomic origin and pristine preservation of these scales, previously overlooked in deep-sea sediments because of their minute size ( $\leq 1 \mu\text{m}$ ), suggest that they were rapidly transported to the sea floor. Eukaryotic scales made of proteins embedded into cellulose and other polysaccharides potentially provide abundant resistant and sticky matter to enhance aggregation and flux of marine snow particles to the deep ocean, contributing to the largely underestimated role of coagulation of small phytoplankters in the biological pump (33). Thus, the tiny haptophytes may have been essential mediators of carbon fluxes from the atmosphere to the deep oceans and the lithosphere throughout much of the Phanerozoic Eon.

## Methods

**Sampling, DNA Extraction, and Construction of LSU rDNA Clone Libraries.** At each sampling station (Fig. S1 and Table S1) 5–15 L of seawater was immediately prefiltered through a 200- $\mu\text{m}$  nylon mesh and collected in an acid-washed carboy. The water was then filtered, using peristaltic pumping, through a 3- $\mu\text{m}$  pore-size Nucleopore polycarbonate filter (Millipore), before recovery of picoplanktonic cells in 0.2- $\mu\text{m}$  pore-size Sterivex filter units (Millipore). Filters were preserved in lysis buffer (40 mM EDTA, 50 mM Tris-HCl, 0.75 M sucrose) and stored at  $-80^\circ\text{C}$  until genomic DNA extraction was performed as in ref. 34. Approximately 1,000 bp nuclear LSU rDNA fragments

including the D1–D2 domains were PCR amplified using the forward haptophyte-specific primer *Hapto\_4* (5'-atggcgaatgaagcggg-3'), and the reverse general eukaryote primer *Euk\_34r* (5'-gcatcgccagttctgtacc-3'). PCR reactions (98 °C for 30 s, 50 °C for 30 s, and 72 °C for 60 s, with initial denaturation and final extension steps) were performed over a maximum of 30 cycles to limit formation of chimeric sequences (35) using the *Phusion* high-fidelity PCR DNA polymerase (New England Biolabs), which is specifically suited for amplification of GC-rich DNA. PCR products were purified using the MinElute gel extraction kit (Qiagen) and 3'-A-overhangs were bound to DNA fragments by adding 0.2 mM dATP, 1 unit of *Taq* DNA polymerase, and 1 $\times$  *Taq* DNA polymerase buffer to the purified PCR product, and incubating for 20 min at 72 °C. Classical TA-cloning into OneShot DH5 $\alpha$ -T1 competent bacteria using the TOPO TA kit (Invitrogen) was then performed according to the manufacturer's instructions. Clone libraries were checked by PCR using the M13 forward and reverse primers and sequencing of  $\approx 25$ –35 random clones in both directions. The entire process of library construction was repeated until  $>85\%$  of white colonies yielded high-quality sequences. Libraries were then sent to High-Throughput Sequencing Solutions ([www.htseq.org](http://www.htseq.org)) for random automatic picking of 200 clones, plasmid minipreps, and automatic sequencing of both strands of 150–200 LSU rDNA fragments per library.

**Molecular Biodiversity, Phylogenetic, Molecular Clock, and Biogeographic Analyses.** The choice of the LSU rDNA D1–D2 fragment over the classically used SSU rDNA to assess haptophyte diversity was motivated by the inability of the latter marker to distinguish closely related species (Table S5). D1–D2 LSU rDNA fragments show virtually no intraspecific variations while discriminating morphospecies that split in the Pleistocene. Unambiguous LSU rDNA sequences were first screened for chimeras using Check-Chimera (36), then double checked by thorough visual inspection of all sequences producing abnormally long branches in neighbor-joining trees (37) as described in Hugenholtz and Huber (38). This conservative approach led to the removal of  $\approx 13\%$  of putative chimeric sequences from subsequent analyses. The remaining 674 environmental sequences were added to 64 nuclear LSU rDNA sequences obtained from taxonomically identified clonal haptophyte cultures from the Roscoff Culture Collection (<http://www.sb-roscoff.fr/Phyto/RCC>), and 3 sequences from GenBank. LSU rDNA sequences were aligned using Muscle (39) and the resulting alignment was manually inspected in Genetic Data Environment 2.2 (40). The Akaike Information Criterion (41) was used to select the most appropriate model of nucleotide substitution: The general time-reversible model plus  $\Gamma_4$  and invariable sites. For each of the libraries, PAUP\* 4.0b10 (42) was used to build pairwise maximum likelihood distance matrices under the model selected above for estimation of rarefaction curves and rDNA richness based on the average neighbor algorithm implemented in DOTUR (43). Phylogenies including both environmental and culture sequences were reconstructed using MrBayes v3.1.2 (44), with 2 independent samplers,  $10^7$  steps, tempering with 1 cold and 3 heated chains, and burn-in of  $10^4$  steps. A Bayesian analysis implemented in BEAST v1.4.6 (45) was performed to construct the phylogeny while estimating divergence times (Fig. S2). This relaxed clock analysis included the 184 sequences from the total alignment that were  $>95\%$  divergent. Absolute time calibration was based on the earliest geological record for the evolution of calcification [i.e.,  $\approx 220$  Mya (46)] and 4 minimum divergence dates derived from stratigraphic data: in the order Coccolithales, the  $\approx 65$ -million-year-old first appearance of the genus *Coccolithus* and the  $\approx 24$ -million-year-old divergence between the genera *Umbilicosphaera* and *Calcidiscus*; in the Syracosphaerales, the  $\approx 55$ -million-year-old split between the genera *Coronosphaera* and *Scyphosphaera/Helicosphaera* and the  $\approx 32$ -million-year-old divergence between the genera *Scyphosphaera* and *Helicosphaera* sensu stricto. Note that the relative branching pattern between the monophyletic groups (Syracosphaera; Coronosphaera), (Helicosphaera; Scyphosphaera), and (Algirosphaera) is not statistically supported and varies depending on reconstruction methods. Minimum ages were constrained with a diffuse prior  $\Gamma(1, 0.15)$  distribution for the onset of calcification and prior  $\Gamma(1, 0.005)$  distributions for the fossil ages. Convergence was checked by running 4 independent samplers with  $10^8$  steps.

**Assessment of the Contribution of Haptophytes to Global Oceanic Photosynthetic Biomass.** The model in ref. 47 was modified and adapted to 19'-hexanoyloxyfucoxanthin (19-Hex), fucoxanthin (Fuco), and zeaxanthin (Zea), the major carotenoids of haptophytes, diatoms, and photosynthetic prokaryotes, respectively. We identified a set of parameters to infer vertical profiles of 19-Hex, Fuco, and Zea for stratified or mixed water conditions, and for any given concentration of surface chlorophyll *a* or  $[\text{Chl}a]_{\text{surf}}$ , based on the following method. Among the  $>2,400$  worldwide HPLC-

<sup>†</sup>Complex mixotrophic regimes may also explain why none of the open ocean haptophytes are currently available in culture collections.

derived pigment profiles, the ones from stratified waters were discriminated from those from well-mixed waters, based on the ratio of the euphotic layer depth  $Z_{eu}$  (the depth at which photosynthetically available radiation is reduced to 1% of its surface value) to the mixed layer depth  $Z_m$ .  $Z_{eu}$  was computed from the vertical profiles of [Chla] using bio-optical models (48, 49), while  $Z_m$  was extracted from the *Levitus* global monthly mean climatology. For both stratified and mixed waters, the vertical profiles of 19-Hex, Fuco, and Zea were sorted into "trophic categories" defined by successive intervals of [Chla]<sub>surf</sub> values. Average profiles were first computed independently for each trophic category and each pigment. Because the average pigment profiles display a deterministic behavior in terms of vertical shape and magnitude along the trophic gradient, they could be modeled and parameterized as a function of [Chla]<sub>surf</sub>. The predictive skill of the parameters was successfully tested using an independent data set (47). Our empirical model was then applied to monthly composites of *SeaWiFS*-derived [Chla]<sub>surf</sub> values for the year 2000, on a pixel-by-pixel basis.  $Z_{eu}$  was first computed from [Chla]<sub>surf</sub> by using the log-log linear relationship linking [Chla]<sub>surf</sub> to the euphotic layer-integrated Chla content (Eq. 8 in ref. 47) and the relationship linking this last parameter to  $Z_{eu}$  (49). The euphotic depth was then compared to the mixed layer depth to determine whether the water column was stratified (i.e.,  $Z_{eu} \geq Z_m$ ) or mixed (i.e.,  $Z_{eu} < Z_m$ ). For stratified waters, [Chla]<sub>surf</sub> was used to produce dimensionless profiles (with respect to depth and biomass) of 19-Hex, Fuco, and Zea, which were then restored to physical units by multiplying depths by  $Z_{eu}$  and concentrations by the average Chla concentration within the euphotic layer. For mixed water conditions, the surface concentration of each pigment was inferred from [Chla]<sub>surf</sub> and extrap-

lated within the euphotic layer to generate uniform vertical profiles. This procedure yielded monthly depth-resolved fields of 19-Hex, Fuco, Zea, and Chla for the world ocean, which were then integrated over the euphotic zone. For each pixel, the resulting monthly 19-Hex, Fuco, and Zea integrated contents were converted into Chla equivalents using the appropriate pigment to Chla ratios determined by multiple regression analysis performed on the global pigment database (47). The obtained monthly Chla biomasses attributed to each group were averaged over the year to estimate annual mean values. These values were normalized to the annual mean euphotic layer-integrated Chla content to determine the relative contribution (%) of each phytoplankton group to the total phytoplankton chlorophyll-based biomass (Fig. 4). Finally, for each of the 3 phytoplankton groups, an annual mean Chla standing stock was calculated as the sum of the annually averaged value of each pixel multiplied by the corresponding pixel surface area. Coastal areas (bathymetry <200 m), large lakes, and inland seas were not considered in this analysis.

**ACKNOWLEDGMENTS.** We thank Swati Narayan-Yadav for practical help to obtain genetic data; Ramon Massana for sharing pico-DNA extractions; Jeremy Young for providing SEM images; and Marie-Pierre Aubry, Paul Falkowski, and David Gruber for critical discussions. This work was supported by National Science Foundation Grants DEB-0415351 and IRES-0652093, an Action Thématique et Incitative sur Programme fellowship from the Centre National de la Recherche Scientifique (to C.d.V.), and the Canadian Natural Sciences and Engineering Research Council (S.A.B.). It is part of the pluridisciplinary project Biodiversity of Open Ocean Microcalcifiers (BOOM), funded by the Institut Français de la Biodiversité via the Agence National de la Recherche, Grant ANR-05-BDIV-004.

- Brocks JJ, Logan GA, Buick R, Summons RE (1999) Archean molecular fossils and the early rise of eukaryotes. *Science* 285:1033–1036.
- Field CB, Behrenfeld MJ, Randerson JT, Falkowski P (1998) Primary production of the biosphere: Integrating terrestrial and oceanic components. *Science* 281:237–240.
- Falkowski PG, Knoll AH (2007) *Evolution of Primary Producers in the Sea* (Elsevier Academic, Amsterdam), p 441.
- Goericke R, Welschmeyer NA (1993) The marine prochlorophyte *Prochlorococcus* contributes significantly to phytoplankton biomass and primary production in the Sargasso Sea. *Deep-Sea Res Part I Oceanogr Res Pap* 40:2283–2294.
- Chisholm SW, et al. (1988) A novel free-living prochlorophyte abundant in the oceanic euphotic zone. *Nature* 334:340–343.
- Kettler GC, et al. (2007) Patterns and implications of gene gain and loss in the evolution of *Prochlorococcus*. *PLoS Genet* 3:e231.
- Li WKW (1995) Composition of ultraphytoplankton in the central North Atlantic. *Mar Ecol Prog Ser* 122:1–8.
- Worden AZ, Nolan JK, Palenik B (2004) Assessing the dynamics and ecology of marine picophytoplankton: The importance of the eukaryotic component. *Limnol Oceanogr* 49:168–179.
- Andersen RA, Bidigare RR, Keller MD, Latasa M (1996) A comparison of HPLC pigment signatures and electron microscopic observations for oligotrophic waters of the North Atlantic and Pacific Oceans. *Deep-Sea Res Stud Oceanogr* 43:517–537.
- Lovejoy C, Massana R, Pedros-Alio C (2006) Diversity and distribution of marine microbial eukaryotes in the Arctic Ocean and adjacent seas. *Appl Environ Microbiol* 72:3085–3095.
- Not F, et al. (2008) Protistan assemblages across the Indian Ocean, with a specific emphasis on the picoeukaryotes. *Deep-Sea Res Part I Oceanogr Res Pap* 55:1456–1473.
- Moon-van der Staay SY, De Wachter R, Vulout D (2001) Oceanic 18S rDNA sequences from picoplankton reveal unsuspected eukaryotic diversity. *Nature* 409:607–610.
- Massana R, et al. (2004) Phylogenetic and ecological analysis of novel marine stramenopiles. *Appl Environ Microbiol* 70:3528–3534.
- Guillou L, et al. (2008) Widespread occurrence and genetic diversity of marine parasitoids belonging to Syndiniales (Alveolata). *Environ Microbiol* 10:3349–3365.
- Vaulot D, Romari K, Not F (2002) Are autotrophs less diverse than heterotrophs in marine picoplankton? *Trends Microbiol* 10:266–267.
- Zubkov MV, Tarran GA (2008) High bacterivory by the smallest phytoplankton in the North Atlantic Ocean. *Nature* 455:224–226.
- Sogin ML, et al. (2006) Microbial diversity in the deep sea and the underexplored "rare biosphere." *Proc Natl Acad Sci USA* 103:12115–12120.
- de Vargas C, Aubry MP, Robert I, Young J (2007) The origin and evolution of coccolithophores: Form coastal hunters to oceanic farmers. *Evolution of Primary Producers in the Sea*, eds Falkowski PG, Knoll AH (Elsevier Academic, Amsterdam), pp 251–286.
- Edwardsen B, et al. (2000) Phylogenetic reconstruction of the Haptophyta inferred from 18S ribosomal DNA sequences and available morphological data. *Phycologia* 39:19–35.
- Edwardsen B, Paasche E (1998) Bloom dynamics and physiology of *Prymnesium* and *Chrysochromulina*. *Physiological Ecology of Harmful Algal Blooms*, eds Anderson DM, Cembella AD, Hallegraeff GM (Springer, Berlin), Vol 41, pp 193–208.
- Falkowski PG, et al. (2004) The evolution of modern eukaryotic phytoplankton. *Science* 305:354–360.
- Fuller NJ, et al. (2006) Molecular analysis of photosynthetic picoeukaryote community structure along an Arabian Sea transect. *Limnol Oceanogr* 51:2502–2514.
- McDonald SM, Sarno D, Scanlan DJ, Zingone A (2007) Genetic diversity of eukaryotic ultraphytoplankton in the Gulf of Naples during an annual cycle. *Aquat Microb Ecol* 50:75–89.
- Worden AZ, Not F (2008) Ecology and diversity of picoeukaryotes. *Microbial Ecology of the Oceans*, ed Kirchman DL (Wiley, Hoboken, NJ), pp 159–205.
- Nygaard K, Tobiesen A (1993) Bacterivory in algae: A survival strategy during nutrient limitation. *Limnol Oceanogr* 38:273–279.
- Tillmann U (1998) Phagotrophy of a plastidic haptophyte, *Prymnesium patelliferum*. *Aquat Microb Ecol* 14:155–160.
- Legrand C, Johansson N, Johnsen G, Børshiem KY, Granéli E (2001) Phagotrophy and toxicity variation in the mixotrophic *Prymnesium patelliferum* (Haptophyceae). *Limnol Oceanogr* 46:1208–1214.
- Kawachi M, Inouye I, Maeda O, Chihara M (1991) The haptonema as a food-capturing device: Observations on *Chrysochromulina hirta* (Prymnesiophyceae). *Phycologia* 30:63–573.
- Aubry M-P (2009) A sea of lilliputians. *Extinction, Dwarfing and the Lilliput Effect*, eds Twitchett R, Wade BS (Palaeogeography, Palaeoclimatology, Palaeoecology, Special Publication), in press.
- Unrein F, Massana R, Alonso-Saez L, Gasol JM (2007) Significant year-round effect of small mixotrophic flagellates on bacterioplankton in an oligotrophic coastal system. *Limnol Oceanogr* 52:456–469.
- Ras J, Claustre H, Uitz J (2008) Spatial variability of phytoplankton pigment distributions in the Subtropical South Pacific Ocean: Comparison between in situ and predicted data. *Biogeosciences* 5:353–369.
- Goody AJ, Esteban GF, Clarke KJ (2006) Organic and siliceous protistan scales in north-east Atlantic abyssal sediments. *J Mar Biol Assoc UK* 86:679–688.
- Richardson TL, Jackson GA (2007) Small phytoplankton and carbon export from the surface ocean. *Science* 315:838–840.
- Diez B, Pedros-Alio C, Massana R (2001) Study of genetic diversity of eukaryotic picoplankton in different oceanic regions by small-subunit rRNA gene cloning and sequencing. *Appl Environ Microbiol* 67:2932–2941.
- Acinas SG, Sarma-Rupavarm R, Klepac-Ceraj V, Polz MF (2005) PCR-induced sequence artifacts and bias: Insights from comparison of two 16S rRNA clone libraries constructed from the same sample. *Appl Environ Microbiol* 71:8966–8969.
- Cole JR, et al. (2003) The Ribosomal Database Project (RDP-II): Previewing a new autoaligner that allows regular updates and the new prokaryotic taxonomy. *Nucleic Acids Res* 31:442–443.
- Saitou N, Nei M (1987) The neighbor-joining method: A new method for reconstructing phylogenetic trees. *Mol Biol Evol* 4:406–425.
- Hughenoltz P, Huber T (2003) Chimeric 16S rDNA sequences of diverse origin are accumulating in the public databases. *Int J Syst Evol Microbiol* 53:289–293.
- Edgar RC (2004) MUSCLE: multiple sequence alignment with high accuracy and high throughput. *Nucleic Acids Res* 32:1792–1797.
- Larsen N, et al. (1993) The ribosomal database project. *Nucleic Acids Res* 21:3021–3023.
- Posada D, Crandall KA (1998) Modeltest: Testing the model of DNA substitution. *Bioinformatics* 14:817–818.
- Swofford DL (2002) PAUP\*: Phylogenetic analysis using parsimony (\*and other methods). Version 4.0b10. (Sinauer, Sunderland, MA).
- Schloss PD, Handelsman J (2005) Introducing DOTUR, a computer program for defining operational taxonomic units and estimating species richness. *Appl Environ Microbiol* 71:1501–1506.

44. Ronquist F, Huelsenbeck JP (2003) MrBayes 3: Bayesian phylogenetic inference under mixed models. *Bioinformatics* 19:1572–1574.
45. Drummond AJ, Ho SYW, Phillips MJ, Rambaut A (2006) Relaxed phylogenetics and dating with confidence. *PLoS Biol* 4:e88.
46. Bown PR, Lees JA, Young JR (2004) Calcareous nannoplankton evolution and diversity through time. *Coccolithophores: From Molecular Process to Global Impact*, eds Thierstein HR, Young JR (Springer, Berlin), pp 481–508.
47. Uitz J, Claustre H, Morel A, Hooker SB (2006) Vertical distribution of phytoplankton communities in open ocean: An assessment based on surface chlorophyll. *Limnol Oceanogr* 111:C08005.
48. Morel A, Berthon JF (1989) Surface pigments, algal biomass profiles, and potential production of the euphotic layer: Relationships reinvestigated in view of remote-sensing applications. *Limnol Oceanogr* 34:1545–1562.
49. Morel A, Maritorena S (2001) Bio-optical properties of oceanic waters: A reappraisal. *Limnol Oceanogr* 106 (C4):7163–7180.
50. Bown PR (2005) Calcareous nannoplankton evolution: A tale of two oceans. *Microplanktonology* 51:299–308.
51. Aubry M-P, Bord D (2009) Reshuffling the cards in the photic zone at the Eocene/Oligocene boundary. *The Late Eocene Earth: Hot House, Ice House, and Impacts*, eds Koeberl C, Montanari A (Geological Society of America, Boulder, CO).